Journal of Solid Mechanics Vol. 12, No. 4 (2020) pp. 791-803
DOI: 10.22034/jsm.2019.1873249.1462

Effect of Vertex Angle on Elastic-Plastic Stability of a Steel Open Conical Shell

H. Shokrollahi *

Department of Mechanical Engineering, Faculty of Engineering, Kharazmi University, Tehran, Iran

Received 9 July 2020; accepted 14 September 2020

ABSTRACT

In this paper, the stability of a conical shell panel in elastic-plastic domain is considered. The shell is made of an isotropic material (316L steel) with linear work hardening behavior. The shell is placed on simply supported end constraints and the acting loads are in the form of longitudinal compressive force and lateral pressure. The incremental Prandtl-Reuss plastic flow theory and von Mises yield criterion are used in the analysis. The problem is formulated based on classical shell theory and nonlinear geometrical strain-displacement relations are assumed. The stability equations are derived using the principle of the stationary potential energy. Using Ritz method the equations are solved and the numerical results obtained for different values of semi vertex and subtended angles. The obtained results show that there is a distinct semi vertex angle in which the shell has the best stability conditions. Also, there will be a limiting condition for the semi vertex angels beyond which the instability will not occur.

Keywords: Elastic-plastic; Buckling; Deformation; Conical shell; Stability.

1 INTRODUCTION

CONICAL shell panels are one of the widely used geometrical shapes in engineering applications, especially in aerospace and marine industries. The stability of shell structures is a very significant problem in both linear and nonlinear analysis of these structures. To reach a good consideration of carrying capacity of the structures, comprehensive understanding of the critical equilibrium under combined loading is needed. The stability analysis of shells developed considerably during the years before. This development is mainly based on the computational techniques. A comprehensive review of works published before 1982 has been presented by Bushnell [1] in which elastic-plastic shell stability analyses and numerical methods were discussed. Zielnica [10] and [11] analyzed elastic-plastic stability problems of conical shells. Paczos and Zielnica [6] investigated the stability of conical panels made of two orthotropic layers. Jaskula and Zielnica [2] and Zielnica [12] presented an analysis for elastic-plastic stability of sandwich cylindrical and conical panels, based on deformation theory of plasticity. To the best knowledge of the authors, there are a few works in the literatures on elastic plastic analysis of conical shell panels.

*Corresponding author. Tel.: +98 26 34579600; Fax: +98 26 34569555.
E-mail address: hshokrollahi@khu.ac.ir (H. Shokrollahi).

However elastic buckling analyses of different conical shells can be found in the literature (Naderi *et al.* [5], Kouchakzadeh and Shakouri [3], Shakouri *et al.* [7]).

The aim of present paper is to investigate the effects of vertex angle of the shell, as a geometric parameter, on its elastic-plastic stability. The shell is made of an isotropic elastic-plastic material (316L steel) with linear work hardening behavior. The end edges of the shell are simply supported and the acting loads are in the form of longitudinal compressive force and lateral pressure. The incremental Prandtl-Reuss plastic flow theory and von Mises yield criterion are used in the analysis. The problem is formulated based on classical shell theory and the geometrical strain-displacement relations are assumed to be nonlinear ones. The stability equations are derived using the principle of the stationary potential energy. Using Ritz method, the equations are solved and the numerical results obtained for different values of semi vertex and subtended angles.

2 PROBLEM DEFINITION AND ASSUMPTIONS

Fig. 1 shows an open conical shell and two different types of loadings acting on it. The acting loads are in the form of a longitudinal compressive force, N, and a uniform lateral pressure, q. According to Fig. 1, β is subtended angle, α is semi vertex angle, R_1 and R_2 are mid-plane smaller and larger radii of two curved ends, respectively, L is the length of the shell and the shell thickness is assumed to be h and constant through the length.

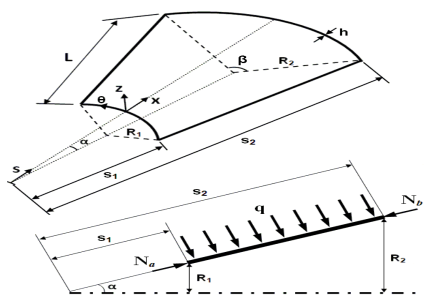

Fig.1
Geometry of the conical shell and applied loading.

3 FORMULATION

3.1 Strain displacement relations

According to classical shell theory (CST), the normal and shear strains of the conical shell are as follows (Soedel [8]):

$$\begin{Bmatrix} \varepsilon_s \\ \varepsilon_\theta \\ \gamma_{s\theta} \end{Bmatrix} = \begin{Bmatrix} \varepsilon_s^0 \\ \varepsilon_\theta^0 \\ \gamma_{s\theta}^0 \end{Bmatrix} + z \begin{Bmatrix} \kappa_s \\ \kappa_\theta \\ \kappa_{s\theta} \end{Bmatrix} \tag{1}$$

where z denotes the shell thickness direction coordinate, ε_s^0 and ε_θ^0 are normal strains at the middle surface, $\gamma_{s\theta}^0$ is shear strain at the middle surface and κ_s , κ_θ and $\kappa_{s\theta}$ are curvatures of the middle surface which can be expressed in terms of the displacement components, as follows (Soedel [8]):

$$\varepsilon_s^0 = \frac{\partial u}{\partial s} + \frac{1}{2}\left(\frac{\partial w}{\partial s}\right)^2 \tag{2a}$$

$$\varepsilon_\theta^0 = \frac{1}{s\sin\alpha}\frac{\partial v}{\partial \theta} + \frac{u}{s} + \frac{w}{s\tan\alpha} + \frac{1}{2s^2\sin^2\alpha}\left(\frac{\partial w}{\partial \theta}\right)^2 \tag{2b}$$

$$\gamma_{s\theta}^0 = \frac{\partial v}{\partial s} - \frac{v}{s} + \frac{1}{s\sin\alpha}\frac{\partial u}{\partial \theta} + \frac{1}{s\sin\alpha}\frac{\partial w}{\partial s}\frac{\partial w}{\partial \theta} \tag{2c}$$

$$\kappa_s = -\frac{\partial^2 w}{\partial s^2} \tag{2d}$$

$$\kappa_\theta = \frac{\cos\alpha}{s^2 \sin^2\alpha}\frac{\partial v}{\partial\theta} - \frac{1}{s}\frac{\partial w}{\partial s} - \frac{1}{s^2 \sin^2\alpha}\frac{\partial^2 w}{\partial\theta^2} \tag{2e}$$

$$\kappa_{s\theta} = -\frac{2}{s\sin\alpha}\frac{\partial^2 w}{\partial s\partial\theta} + \frac{2}{s^2\sin\alpha}\frac{\partial w}{\partial\theta} + \frac{1}{s\tan\alpha}\frac{\partial v}{\partial s} - \frac{2v}{s^2\tan\alpha} \tag{2f}$$

where u, v, and w represent the displacements of the middle surface of the conical shell in the s, θ, and z directions, respectively. In addition, the subscripts s and θ denote the meridional and circumferential directions, respectively.

3.2 Stress-strain relations

The material stress-strain curve is shown in Fig. 2. The stress-strain curve in infinitesimal strain range is presented by a bilinear model. According to von Mises yield criterion with associated flow rule, plastic strain increment is defined as (Washizu [9]):

$$\delta\varepsilon^p = \frac{3}{2}\frac{\delta\varepsilon_e^p}{\sigma_e}S \tag{3}$$

where ε^p is the plastic strain, ε_e^p is the equivalent plastic strain, σ_e is the equivalent stress and S is the deviatoric stress. The changes in stresses for an isotropic material are defined by following equations (Jaskula and Zielnica [2]),

$$\delta\sigma_s = \frac{E}{\left(1-\nu^2\right)}\left\{\delta\varepsilon_s + \nu\delta\varepsilon_\theta - \frac{\delta\varepsilon_e^p}{2\sigma_e}\left[\left(2-\nu\right)\sigma_s + \left(2\nu-1\right)\sigma_\theta\right]\right\} \tag{4a}$$

$$\delta\sigma_\theta = \frac{E}{\left(1-\nu^2\right)}\left\{\delta\varepsilon_\theta + \nu\delta\varepsilon_s - \frac{\delta\varepsilon_e^p}{2\sigma_e}\left[\left(2-\nu\right)\sigma_\theta + \left(2\nu-1\right)\sigma_s\right]\right\} \tag{4b}$$

$$\delta\tau_{s\theta} = \frac{E}{2\left(1+\nu\right)}\left(\delta\gamma_{s\theta} - 3\frac{\delta\varepsilon_e^p}{\sigma_e}\tau_{s\theta}\right) \tag{4c}$$

where E and ν are the Young's modulus and Poisson's ratio, respectively. For elastic deformation the equivalent plastic strain change, $\delta\varepsilon_e^p$, is set to zero, and with plastic deformation it can be determined according to hardening behaviour of material. Using linear strain hardening (see Appendix A) results as:

$$\delta\varepsilon_e^p = \left(\frac{1}{E_t} - \frac{1}{E}\right)\delta\sigma_e \tag{5}$$

where E_t is the tangent modulus in the plastic range and σ_e is effective stress, defined by:

$$\sigma_e = \sqrt{\sigma_s^2 - \sigma_s\sigma_\theta + \sigma_\theta^2 + 3\tau_{s\theta}^2} \tag{6}$$

Substituting $\delta\varepsilon_e^p$ from Eq. (5) into Eqs. (4) and solving the system of equations for stress variations leads to following equation,

$$\begin{Bmatrix} \delta\sigma_s \\ \delta\sigma_\theta \\ \delta\tau_{s\theta} \end{Bmatrix} = \begin{bmatrix} C_{11} & C_{12} & C_{13} \\ C_{21} & C_{22} & C_{23} \\ C_{31} & C_{32} & C_{33} \end{bmatrix} \begin{Bmatrix} \delta\varepsilon_s \\ \delta\varepsilon_\theta \\ \delta\gamma_{s\theta} \end{Bmatrix} \tag{7}$$

In which the C_{ij} (i, j= 1, 2, 3) are as follows:

$$C_{11} = E\left\{4E_t\left(1+\nu\right)\sigma_e^2 + (E-E_t)\left[18\tau_{s\theta}^2 + \left(1+\nu\right)\sigma_s^2 - 4\left(1+\nu\right)\sigma_s\sigma_\theta + 4\left(1+\nu\right)\sigma_\theta^2\right]\right\}/\psi \tag{8a}$$

$$C_{12} = C_{21} = E\{4E_t\nu\left(1+\nu\right)\sigma_e^2 + (E-E_t)\left[18\nu\tau_{s\theta}^2 + 2\left(1+\nu\right)\sigma_s^2 - 5\left(1+\nu\right)\sigma_s\sigma_\theta + 2\left(1+\nu\right)\sigma_\theta^2\right]\}/\psi \tag{8b}$$

$$C_{13} = C_{31} = 3E\,\tau_{s\theta}\left(E-E_t\right)\left[\left(\nu-2\right)\sigma_s + \left(1-2\nu\right)\sigma_\theta\right]/\psi \tag{8c}$$

$$C_{22} = E\left\{4E_t\left(1+\nu\right)\sigma_e^2 + (E-E_t)\left[18\tau_{s\theta}^2 + 4\left(1+\nu\right)\sigma_s^2 - 4\left(1+\nu\right)\sigma_s\sigma_\theta + \left(1+\nu\right)\sigma_\theta^2\right]\right\}/\psi \tag{8d}$$

$$C_{23} = C_{32} = 3E\,\tau_{s\theta}\left(E-E_t\right)\left[\left(1-2\nu\right)\sigma_s + \left(\nu-2\right)\sigma_\theta\right]/\psi \tag{8e}$$

$$C_{33} = \frac{E}{2}\{4E_t\left(1-\nu^2\right)\sigma_e^2 + (E-E_t)[\left(5-4\nu\right)\sigma_s^2 - 2\left(4-5\nu\right)\sigma_s\sigma_\theta + \left(5-4\nu\right)\sigma_\theta^2\}/\psi \tag{8f}$$

$$\psi = \left(1+\nu\right)\left\{4E_t\left(1-\nu^2\right)\sigma_e^2 + (E-E_t)\left[18\left(1-\nu\right)\tau_{s\theta}^2 + \left(5-4\nu\right)\sigma_s^2 - 2\left(4-5\nu\right)\sigma_s\sigma_\theta + \left(5-4\nu\right)\sigma_\theta^2\right]\right\} \tag{8g}$$

The stresses resulted from the external loadings (Fig. 1) in pre-buckling state of stress are as follows:

$$\sigma_s = \frac{q\,s\,tan\,\alpha}{2h}\left[\left(\frac{s_1}{s}\right)^2 - 1\right] - \frac{N_a s_1}{s\,h} \tag{9a}$$

$$\sigma_\theta = -\frac{q\,s\,tan\,\alpha}{h} \tag{9b}$$

$$\tau_{s\theta} = 0 \tag{9c}$$

It is assumed that the loading parameters, q and N_a, are dependent. The following parameter η, is introduced as the ratio of lateral to longitudinal load

$$\eta = \frac{N_a}{qR_1} \tag{10}$$

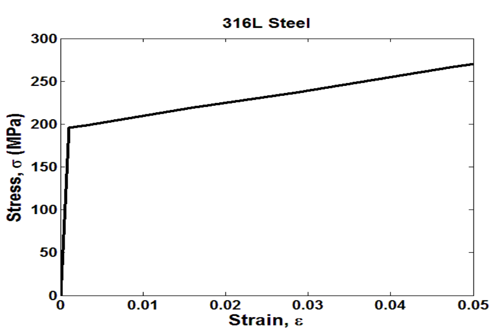

Fig.2
Stress-strain curve for 316L steel (Lee *et al.* [4])

4 STABILITY EQUATIONS AND SOLUTION PROCEDURE

The principle of the stationary potential energy which is correct for both the pre- and post-critical deformation, states that,

$$\delta\Pi = \delta\left(U - W\right) = 0 \tag{11}$$

where Π, U and W are the total potential energy, deformation energy and the work done by the external loadings, respectively.

The deformation energy and the work done by the external loadings can be expressed as following (Washizu [9]),

$$U = \frac{\sin\alpha}{2}\int_{-h/2}^{h/2}\int_{0}^{\beta}\int_{s_1}^{s_2}\left(C_{11}\varepsilon_s^2 + 2C_{12}\varepsilon_s\varepsilon_\theta + C_{22}\varepsilon_\theta^2 + C_{33}\gamma_{s\theta}^2\right)s\,ds\,d\theta\,dz \tag{12}$$

$$W = \frac{1}{2}N_a s_1 \sin\alpha\int_{0}^{\beta}\int_{s_1}^{s_2}\left(\frac{\partial w}{\partial s}\right)^2 ds\,d\theta + q\sin\alpha\int_{0}^{\beta}\int_{s_1}^{s_2} w\,s\,ds\,d\theta \tag{13}$$

Having on hand the U and W in terms of displacement components, one can establish the expression for the total potential energy. Implementing Eq. (11) following equation is obtained,

$$\begin{aligned}
&\int_{0}^{\beta}\int_{s_1}^{s_2}(\underline{Eq1}\,\delta u + \underline{Eq2}\,\delta v + \underline{Eq3}\,\delta w)\,ds\,d\theta \\
&+\int_{s_1}^{s_2}(\underline{BC\theta u}\,\delta u + \underline{BC\theta v}\,\delta v + \underline{BC\theta w}\,\delta w + \underline{BC\theta dw}\,\delta\frac{\partial w}{\partial\theta})\,ds \\
&+\int_{0}^{\beta}(\underline{BCsu}\,\delta u + \underline{BCsv}\,\delta v + \underline{BCsw}\,\delta w + \underline{BCsdw}\,\delta\frac{\partial w}{\partial s})\,d\theta + \underline{BCs\theta}\,\delta w = 0
\end{aligned} \tag{14}$$

The terms in Eq. (14) are presented as Appendix B. As can be seen the obtained equations are highly nonlinear and a large computation effort is needed to solve these equations directly. However, an alternative solution procedure is used here to define unstable regions for conical shells, as presented here.

Introducing approximate functions for the displacements with unknown coefficients A_i and using Ritz method, leads to the following equations,

$$\frac{\partial\Pi}{\partial A_i} = 0 \tag{15}$$

Application of Eq. (15) on the obtained potential energy leads to a system of nonlinear equations in terms of unknown coefficients A_i. Solving these equations will give the displacement components in the considered shell. The shell is assumed to be simply supported at all the edges. Geometric boundary conditions for simply supported conical shell are as follows:

$$\begin{aligned} &u = w = 0; \quad \theta = 0, \beta \\ &v = w = 0 \quad s = s_1, s_2 \end{aligned} \tag{16}$$

To satisfy the boundary conditions (16), based on Ritz method, the following approximate functions for the displacements are introduced (Paczos and Zielnica [6]):

$$u\left(s,\theta\right) = A_1 s^2 \sin^2\alpha\cos\frac{m\pi\left(s - s_1\right)}{L}\sin\frac{n\pi\theta}{\beta} \tag{17a}$$

$$v\left(s,\theta\right)=A_2 s^2 \sin^2\alpha \sin\frac{m\pi\left(s-s_1\right)}{L}\cos\frac{n\pi\theta}{\beta} \tag{17b}$$

$$w\left(s,\theta\right)=A_3 s^2 \sin^2\alpha \sin\frac{m\pi\left(s-s_1\right)}{L}\sin\frac{n\pi\theta}{\beta} \tag{17c}$$

where A_1, A_2 and A_3 are unknown coefficients and m and n are axial and circumferential half-wave numbers, respectively. By comprising Π the total potential energy and then using the minimization principle by Eq. (15) that is setting the partial derivatives of the total potential energy with respect to unknown coefficients A_i (i=1,2,3) to zero, a set of three nonlinear equations in terms of unknown parameters A_1, A_2 and A_3, is obtained as follows:

$$f_{11}A_1+f_{12}A_2+f_{13}A_3+f_{14}A_3^2=0 \tag{18a}$$

$$f_{21}A_1+f_{22}A_2+f_{23}A_3+f_{24}A_3^2=0 \tag{18b}$$

$$f_{31}A_1+f_{32}A_2+\left(f_{33}+q\eta\tilde{f}_{33}\right)A_3+f_{34}A_3^2+f_{35}A_3^3+f_{36}A_1A_3+f_{37}A_2A_3+qf_{38}=0 \tag{18c}$$

where coefficients f_{11}, f_{12}, …, f_{38} and $\tilde{f}_{33}$ are very lengthy and for the sake of brevity they will not be given here. These coefficients depend on geometrical and material parameters of the shell as well as the assumed half-wave numbers m and n. Solving the above set of equations for q leads to

$$q=\frac{e_1A_3+e_2A_3^2+e_3A_3^3}{e_4+e_5\eta A_3} \tag{19}$$

where η is defined by Eq. (10). Note that the expressions for the coefficients e_i (i=1,…,5) are very lengthy and for the sake of brevity they will not be given here. The coefficients in Eq. (19) depend on the loading parameters q and η. Therefore by using an iterative method the critical values of loading are obtained. To this aim, we implement an iterative procedure similar to one introduced by Paczos and Zielnica [6], which is described briefly in the following. Primarily, the geometrical parameters (R_1, L, h, α, β) and materials constants are defined. Then the ratio of axial load to lateral pressure (η) is assumed. Now for sequential values of A_3 the corresponding loadings are calculated by using an iterative method in which at k^{th} iteration, using Eq. (19) the value of q are calculated as follows:

$$q^{(k)}=\frac{e_1^{(k-1)}A_3+e_2^{(k-1)}A_3^2+e_3^{(k-1)}A_3^3}{e_4^{(k-1)}+e_5^{(k-1)}\eta A_3} \tag{20}$$

Then the next iteration started by updating q and coefficients depending on it. The calculations are repeated until the convergence of q is achieved. The result of above procedure is the determination of external load values (q and N_a) as functions of shell deflection.

Note that the proposed method with appropriate modification can be applied to other types of loadings. For example for q=0, Eq. (19) can be replaced by following equation

$$N_a=\frac{e_1A_3+e_2A_3^2+e_3A_3^3}{\overline{e}_5A_3} \tag{21}$$

Moreover, the above mentioned procedure can be repeated for finding N_a as a function of shell deflection. It should be further noted that the principle of the stationary potential energy, and hence the presented analysis, is valid only if the loading is maintained constant during the deformation.

Based on the above outlined procedure and by aids of the MATLAB program solver a self-developed computer program is written by which the external load values (q and N_a) as functions of shell deflection, and the critical values of loading can be obtained. It should be emphasized that the presented procedure is an effective technique to define unstable regions for conical shells.

5 RESULTS AND DISCUSSIONS

A conical shell panel made of 316L steel, whose stress-strain curve is shown in Fig. 2, was considered for numerical calculations. The assumed value of the yield strength of 316L steel is 196 *MPa* and other material parameters are $E = 193$ *GPa*, $v = 0.29$ and $E_t = 1.5$ *GPa*. The shell geometrical parameters are considered such that the instability occurs beyond the elastic limit of the shell material. It must be emphasized that the geometrical parameters also were chosen in a way that the instability occurs in the range of applicability of the infinitesimal theory of plasticity. In order to investigate the validity of the obtained results, a sample problem is solved using both the present solution method and finite element method (FEM). To this aim a conical shell panel made of 316L steel subjected to a uniform lateral loading ($\eta = 0$) is considered. The geometrical parameters are: $R_1 = 1.2$ *m*, $L = 0.4$ *m*, $h = 5$ *mm*, $\alpha = 45°$, $\beta = 20°$. The variations of the lateral uniform loading versus the maximum lateral deflection of the considered shell panel are shown in Fig. 3 using both present formulation and FEM. The results show that there is a good agreement between FEM results and the obtained results using present formulation.

It is to be mentioned that in constructing the FE model, the ANSYS software (version 16) has been used. The FE model comprises 3,990 3D 20-node brick type elements with total number of 28,618 nodes. Elastic linearly plastic material is defined for the material of the shell. The static analyses are done in the software. It is to be noted that the shell are modeled as a 3D solid, so that no restricting assumptions such as neglecting the out-of- plane stresses in the shell are imposed in finite element modeling.

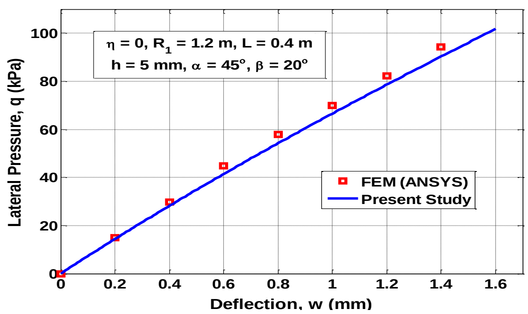

Fig.3
Lateral pressure versus deflection of the shell (calculated at $s = (s_1+s_2)/2$ and $\theta = \beta/2$). Present study and finite element method (FEM).

The assumed geometrical parameters for further studies are: $R_1 = 1.2$ *m*, $L = 0.4$ *m*, $h = 5$ *mm*, $\alpha = 10°$-$60°$, $\beta = 35°$-$45°$. Based on these geometrical representations the variation of lateral pressure vs. shell deflection is shown in Fig. 4 for different ratios of axial load to lateral pressure (η). As shown in Fig. 4, for small η the instability does not occur. By gradually increasing the value of η, the instability initiates at a certain level of loading. As shown in Fig. 4, by increasing the value of η to about 300 the instability occurs. The value of loading in which instability occurs is identified as critical value. The geometrical parameters including the semi vertex angle will affect the stability of the shell, which will be discussed in the following. Note that all the curves shown in Fig. 4 are representative of the elastic-plastic deformation of the shell, because the effective stress defined by Eq. (6) is greater than the yield stress beyond specific values of loadings in each case.

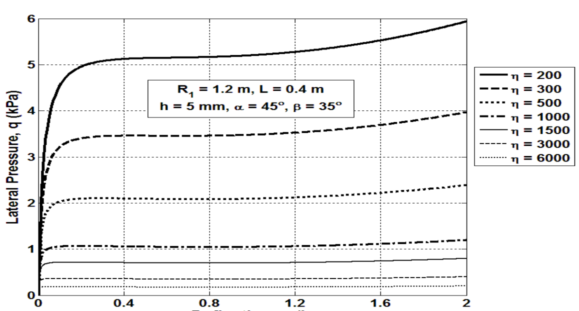

Fig.4
Lateral pressure versus deflection of the shell (calculated at $s = (s_1+s_2)/2$ and $\theta = \beta/2$).

The result of axial load variation vs. shell deflection is shown in Fig. 5 for different values of η. Again, the instability appears by increasing value of η. This figure shows that the axial load, unlike the lateral pressure, will not severely change by increasing the value of η. Also for large values of η>6000 the undistinguishable changes can be seen in the equilibrium curve that is all curves will overlay on top of each others.

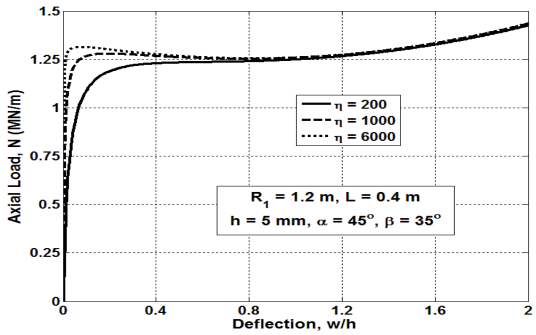

Fig.5
Axial load versus deflection of the shell (calculated at $s = (s_1+s_2)/2$ and $\theta = \beta/2$).

The variation of critical lateral pressure versus variation of semi vertex angle for a shell with $R_1 = 1.2$ *m*, $L = 0.4$ *m*, $h = 5$ *mm*, $\beta = 35°$ is shown in Fig. 6. As shown in this figure, for all values of η there is a distinct semi vertex angle in which the critical lateral pressure has a maximum value. That is the maximum critical pressure is obtained at semi vertex angle of about 23°. One can conclude that this semi vertex angle will give the best elastic-plastic stability for the shell panel with specified parameters and subjected to loading with large values of η.

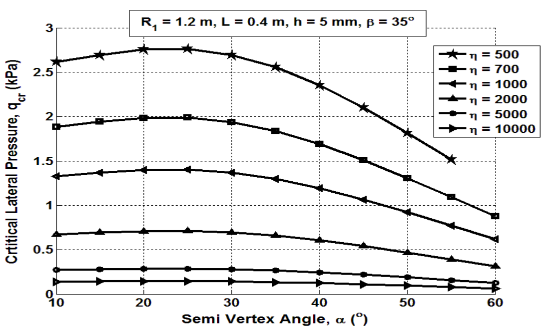

Fig.6
Critical lateral pressure versus semi vertex angle for different values of axial to lateral load ratio.

For the same geometrical parameter given in the above case, the variation of the critical axial loads vs. variation of semi vertex angle for different values of η is shown in Fig. 7. The semi vertex angle related to the maximum critical axial load in this case again is 23° that is the same as in the case of critical pressure shown in Fig. 6. As shown in Fig. 7, for small values of η say 200, there is a limiting value for semi vertex angle (35°), beyond which the instability does not occur.

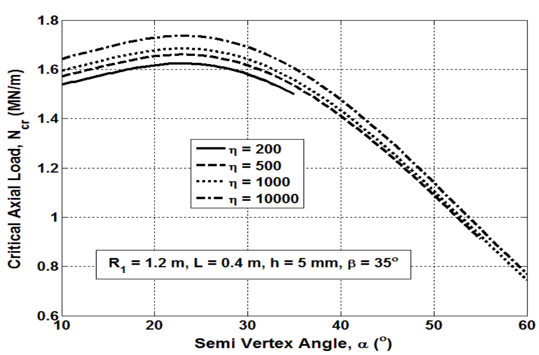

Fig.7
Critical axial load versus semi vertex angle for different values of axial to lateral load ratio.

The dependency of the critical loads to semi vertex angle for a shell with $R_1 = 1.2$ *m*, $L = 0.4$ *m*, $h = 5$ *mm*, $\eta = 10000$ under different values of subtended angle is shown in Fig. 8. As shown in this figure, by increasing the subtended angle the maximum value of q_{cr}-α curve will shift to the right. In the case for the subtended shell angles of 35, 37, 40 and 45°, the maximum critical lateral pressure will be obtained for semi vertex angles of 23.0, 25.5, 28 and 30.3°, respectively. In the results shown in this figure, for the subtended shell angles of 45° there will be a limiting condition for the semi vertex angels beyond which the instability will not occur.

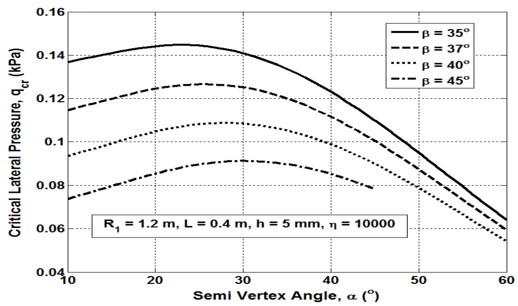

Fig.8
Critical lateral pressure versus semi vertex angle for different values of subtended angle.

6 CONCLUSION

The effects of vertex angle of the conical shell, as a geometric parameter, on its elastic-plastic stability are investigated. The shell is made of 316L steel which is an isotropic elastic-plastic material with linear work hardening behavior. The edges of the shell are simply supported and the acting loads are in the form of longitudinal compressive force and lateral pressure. The incremental Prandtl-Reuss plastic flow theory and von Mises yield criterion are used in the analysis. The problem is formulated based on classical shell theory (the Kirchhoff-Love assumptions) and the geometrical strain-displacement relations are assumed to be nonlinear ones. The stability equations are derived using the principle of the stationary potential energy. Using Ritz method, the equations are solved and the numerical results obtained for different values of semi vertex and subtended angles. Based on this study, it is concluded that there is a distinct semi vertex angle in which the shell has the best elastic-plastic stability conditions. Moreover, for specified shell geometrical and loading parameters there will be a limiting condition for the semi vertex angels beyond which the instability will not occur.

APPENDIX A

For a linear strain hardening material, equivalent stress σ_e is defined by:

$$\sigma_e = \sigma_{y0} + H\varepsilon_e^p \quad \text{(A.1)}$$

where σ_{y0} is the initial yield stress and H is the plasticity (or hardening) modulus. Then the plastic work increment δW^p is:

$$\delta W^p = \sigma_e \delta\varepsilon_e^p \quad \text{(A.2)}$$

From Eq. (A.1) it can be concluded that

$$\delta\varepsilon_e^p = \frac{\delta\sigma_e}{H} \quad \text{(A.3)}$$

On the other hand, the plastic strain increment can be obtained from additive decomposition, as follows:

$$\delta\varepsilon_e^p = \delta\varepsilon_e - \delta\varepsilon_e^e = \frac{\delta\sigma_e}{E_t} - \frac{\delta\sigma_e}{E} = \left(\frac{1}{E_t} - \frac{1}{E}\right)\delta\sigma_e \quad \text{(A.4)}$$

Substituting $\delta\varepsilon_e^p$ from Eq. (A.3) into Eq. (A.4) leads to following equation, for hardening modulus.

$$H = \frac{E_t E}{E - E_t} \quad \text{(A.5)}$$

APPENDIX B

$$\underline{Eq1} = \underline{Eq1}^{L} + \underline{Eq1}^{NL};\ \ \underline{Eq2} = \underline{Eq2}^{L} + \underline{Eq2}^{NL};\ \ \underline{Eq3} = \underline{Eq3}^{L} + \underline{Eq3}^{NL}$$

$$\underline{BCsu} = \underline{BCsu}^{L} + \underline{BCsu}^{NL};\ \ \underline{BCsv} = \underline{BCsv}^{L} + \underline{BCsv}^{NL};\ \ \underline{BCsw} = \underline{BCsw}^{L} + \underline{BCsw}^{NL}$$

$$\underline{BC\theta u} = \underline{BC\theta u}^{L} + \underline{BC\theta u}^{NL};\ \ \underline{BC\theta v} = \underline{BC\theta v}^{L} + \underline{BC\theta v}^{NL};\ \ \underline{BC\theta w} = \underline{BC\theta w}^{L} + \underline{BC\theta w}^{NL}$$

$$\begin{aligned}\underline{Eq1}^{L}:&\frac{C_{22}h\sin\alpha}{s}u-\frac{C_{23}h\sin\alpha}{s}v-\frac{C_{22}h\cos\alpha}{s}w-C_{11}h\sin\alpha\frac{\partial u}{\partial s}+C_{23}h\sin\alpha\frac{\partial v}{\partial s}+C_{12}h\cos\alpha\frac{\partial w}{\partial s}\\&+\frac{(C_{22}+C_{33})h}{s}\frac{\partial v}{\partial\theta}+\frac{C_{23}h\cot\alpha}{s}\frac{\partial w}{\partial\theta}-C_{11}hs\sin\alpha\frac{\partial^2 u}{\partial s^2}-C_{13}hs\sin\alpha\frac{\partial^2 v}{\partial s^2}-2C_{13}h\frac{\partial^2 u}{\partial s\partial\theta}\\&-(C_{12}+C_{33})h\frac{\partial^2 v}{\partial s\partial\theta}-\frac{C_{33}h\csc\alpha}{s}\frac{\partial^2 u}{\partial\theta^2}-\frac{C_{23}h\csc\alpha}{s}\frac{\partial^2 v}{\partial\theta^2}\end{aligned}\tag{B.1}$$

$$\begin{aligned}\underline{Eq1}^{NL}:&\frac{1}{2}(C_{12}-C_{11})h\sin\alpha\left(\frac{\partial w}{\partial s}\right)^2+\frac{C_{23}h}{s}\frac{\partial w}{\partial\theta}\frac{\partial w}{\partial s}+\frac{(C_{12}+C_{22})h\csc\alpha}{2s^2}\left(\frac{\partial w}{\partial\theta}\right)^2-\frac{(C_{12}+C_{33})h\csc\alpha}{s}\frac{\partial w}{\partial\theta}\frac{\partial^2 w}{\partial s\partial\theta}\\&-2C_{13}h\frac{\partial^2 w}{\partial s\partial\theta}\frac{\partial w}{\partial s}-C_{13}h\frac{\partial w}{\partial\theta}\frac{\partial^2 w}{\partial s^2}-C_{11}hs\sin\alpha\frac{\partial w}{\partial s}\frac{\partial^2 w}{\partial s^2}-\frac{C_{23}h(\csc\alpha)^2}{s^2}\frac{\partial w}{\partial\theta}\frac{\partial^2 w}{\partial\theta^2}-\frac{C_{33}h\csc\alpha}{s}\frac{\partial^2 w}{\partial\theta^2}\frac{\partial w}{\partial s}\end{aligned}\tag{B.2}$$

$$\underline{BCsu}^{L}:C_{12}h\sin\alpha u-C_{13}h\sin\alpha v-C_{12}h\cos\alpha w+C_{13}h\frac{\partial u}{\partial\theta}+C_{12}h\frac{\partial v}{\partial\theta}+C_{11}hs\sin\alpha\frac{\partial u}{\partial s}+C_{13}hs\sin\alpha\frac{\partial v}{\partial s}\tag{B.3}$$

$$\underline{BCsu}^{NL}:\frac{C_{12}h\csc\alpha}{2s}\left(\frac{\partial w}{\partial\theta}\right)^2+C_{13}h\frac{\partial w}{\partial\theta}\frac{\partial w}{\partial s}+\frac{1}{2}C_{11}hs\sin\alpha\left(\frac{\partial w}{\partial s}\right)^2\tag{B.4}$$

$$\underline{BC\theta u}^{L}:\frac{C_{23}h}{s}u-\frac{C_{33}h}{s}v-\frac{C_{23}h\cot\alpha}{s}w+\frac{C_{33}h\csc\alpha}{s}\frac{\partial u}{\partial\theta}+\frac{C_{23}h\csc\alpha}{s}\frac{\partial v}{\partial\theta}+C_{13}h\frac{\partial u}{\partial s}+C_{33}h\frac{\partial v}{\partial s}\tag{B.5}$$

$$\underline{BC\theta u}^{NL}:\frac{C_{23}h(\csc\alpha)^2}{2s^2}\left(\frac{\partial w}{\partial\theta}\right)^2+\frac{C_{33}h\csc\alpha}{s}\frac{\partial w}{\partial\theta}\frac{\partial w}{\partial s}+\frac{1}{2}C_{13}h\left(\frac{\partial w}{\partial s}\right)^2\tag{B.6}$$

$$\begin{aligned}\underline{Eq2}^{L}:&-\frac{C_{23}h\sin\alpha}{s}u+\frac{C_{33}h\sin\alpha}{s}v+\frac{C_{23}h\cos\alpha}{s}w-\frac{(C_{22}+C_{33})h}{s}\frac{\partial u}{\partial\theta}+\frac{C_{23}h^3(\cot\alpha)^2}{6s^3}\frac{\partial v}{\partial\theta}+\frac{C_{22}h\cot\alpha}{s}\frac{\partial w}{\partial\theta}\\&-(2C_{13}+C_{23})h\sin\alpha\frac{\partial u}{\partial s}+\left(\frac{C_{33}h^3\cos\alpha\cot\alpha}{12s^2}-C_{33}h\sin\alpha\right)\frac{\partial v}{\partial s}+\left(C_{23}h\cos\alpha-\frac{C_{23}h^3\cos\alpha}{12s^2}\right)\frac{\partial w}{\partial s}\\&+\left(\frac{C_{23}h^3\cot\alpha\csc\alpha}{6s^3}-\frac{C_{22}h^3\cot\alpha}{12s^2}\right)\frac{\partial^2 w}{\partial s\partial\theta}-\frac{(2C_{13}+C_{23})h^3\cos\alpha}{12s}\frac{\partial^2 w}{\partial s^2}-(C_{12}+C_{33})h\frac{\partial^2 u}{\partial s\partial\theta}\\&-2C_{23}\left(h+\frac{h^3(\cot\alpha)^2}{12s^2}\right)\frac{\partial^2 v}{\partial s\partial\theta}-C_{13}hs\sin\alpha\frac{\partial^2 u}{\partial s^2}-\left(\frac{C_{33}h^3\cos\alpha\cot\alpha}{12s}+C_{33}hs\sin\alpha\right)\frac{\partial^2 v}{\partial s^2}\\&-\frac{C_{23}h^3\cot\alpha\csc\alpha}{4s^2}\frac{\partial^3 w}{\partial s\partial\theta^2}-\frac{(C_{12}+2C_{33})h^3\cot\alpha}{12s}\frac{\partial^3 w}{\partial s^2\partial\theta}-\frac{1}{12}C_{13}h^3\cos\alpha\frac{\partial^3 w}{\partial s^3}\\&-\frac{C_{23}h\csc\alpha}{s}\frac{\partial^2 u}{\partial\theta^2}-\left(\frac{C_{22}h\csc\alpha}{s}+\frac{C_{22}h^3(\cot\alpha)^2\csc\alpha}{12s^3}\right)\frac{\partial^2 v}{\partial\theta^2}-\frac{C_{22}h^3\cot\alpha(\csc\alpha)^2}{12s^3}\frac{\partial^3 w}{\partial\theta^3}\end{aligned}\tag{B.7}$$

$$\begin{aligned}\underline{Eq2}^{NL}:&-\frac{C_{33}h}{s}\frac{\partial w}{\partial\theta}\frac{\partial w}{\partial s}-C_{13}h\sin\alpha\left(\frac{\partial w}{\partial s}\right)^2-\frac{2C_{23}h\csc\alpha}{s}\frac{\partial w}{\partial\theta}\frac{\partial^2 w}{\partial s\partial\theta}-(C_{33}h+C_{12}h)\frac{\partial w}{\partial s}\frac{\partial^2 w}{\partial s\partial\theta}-C_{33}h\frac{\partial w}{\partial\theta}\frac{\partial^2 w}{\partial s^2}\\&-C_{13}hs\sin\alpha\frac{\partial w}{\partial s}\frac{\partial^2 w}{\partial s^2}-\frac{C_{22}h(\csc\alpha)^2}{s^2}\frac{\partial w}{\partial\theta}\frac{\partial^2 w}{\partial\theta^2}-\frac{C_{23}h\csc\alpha}{s}\frac{\partial^2 w}{\partial\theta^2}\frac{\partial w}{\partial s}\end{aligned}\tag{B.8}$$

$$\begin{aligned}\underline{BCsv}^{L}:\ & C_{23}h\sin\alpha u-\left(\frac{C_{33}h^{3}\cos\alpha\cot\alpha}{6s^{2}}+C_{33}h\sin\alpha\right)v-C_{23}h\cos\alpha w+C_{33}h\frac{\partial u}{\partial\theta}+\left(C_{23}h+\frac{C_{23}h^{3}\left(\cot\alpha\right)^{2}}{12s^{2}}\right)\frac{\partial v}{\partial\theta}\\ & -\frac{C_{33}h^{3}\cot\alpha}{6s^{2}}\frac{\partial w}{\partial\theta}+C_{13}hs\sin\alpha\frac{\partial u}{\partial s}+\left(\frac{C_{33}h^{3}\cos\alpha\cot\alpha}{12s}+C_{33}hs\sin\alpha\right)\frac{\partial v}{\partial s}+\frac{C_{23}h^{3}\cos\alpha}{12s}\frac{\partial w}{\partial s}\\ & +\frac{C_{23}h^{3}\cot\alpha\csc\alpha}{12s^{2}}\frac{\partial^{2}w}{\partial\theta^{2}}+\frac{C_{33}h^{3}\cot\alpha}{6s}\frac{\partial^{2}w}{\partial s\partial\theta}+\frac{1}{12}C_{13}h^{3}\cos\alpha\frac{\partial^{2}w}{\partial s^{2}}\end{aligned}\tag{B.9}$$

$$\underline{BCsv}^{NL}:\frac{C_{23}h\csc\alpha}{2s}\left(\frac{\partial w}{\partial\theta}\right)^{2}+C_{33}h\frac{\partial w}{\partial\theta}\frac{\partial w}{\partial s}+\frac{1}{2}C_{13}hs\sin\alpha\left(\frac{\partial w}{\partial s}\right)^{2}\tag{B.10}$$

$$\begin{aligned}\underline{BC\theta v}^{L}:\ & \frac{C_{22}h}{s}u-\left(\frac{C_{23}h}{s}+\frac{C_{23}h^{3}\left(\cot\alpha\right)^{2}}{6s^{3}}\right)v-\frac{C_{22}h\cot\alpha w}{s}+\frac{C_{23}h\csc\alpha}{s}\frac{\partial u}{\partial\theta}+\left(\frac{C_{22}h\csc\alpha}{s}+\frac{C_{22}h^{3}\left(\cot\alpha\right)^{2}\csc\alpha}{12s^{3}}\right)\frac{\partial v}{\partial\theta}\\ & -\frac{C_{23}h^{3}\cot\alpha\csc\alpha}{6s^{3}}\frac{\partial w}{\partial\theta}+\frac{C_{22}h^{3}\cot\alpha\left(\csc\alpha\right)^{2}}{12s^{3}}\frac{\partial^{2}w}{\partial\theta^{2}}+C_{12}h\frac{\partial u}{\partial s}+\left(C_{23}h+\frac{C_{23}h^{3}\left(\cot\alpha\right)^{2}}{12s^{2}}\right)\frac{\partial v}{\partial s}\\ & +\frac{C_{22}h^{3}\cot\alpha}{12s^{2}}\frac{\partial w}{\partial s}+\frac{C_{23}h^{3}\cot\alpha\csc\alpha}{6s^{2}}\frac{\partial^{2}w}{\partial s\partial\theta}+\frac{C_{12}h^{3}\cot\alpha}{12s}\frac{\partial^{2}w}{\partial s^{2}}\end{aligned}\tag{B.11}$$

$$\underline{BC\theta v}^{NL}:\frac{C_{22}h\left(\csc\alpha\right)^{2}}{2s^{2}}\left(\frac{\partial w}{\partial\theta}\right)^{2}+\frac{C_{23}h\csc\alpha}{s}\frac{\partial w}{\partial\theta}\frac{\partial w}{\partial s}+\frac{1}{2}C_{12}h\left(\frac{\partial w}{\partial s}\right)^{2}\tag{B.12}$$

$$\begin{aligned}\underline{Eq3}^{L}:\ & -qs\sin\alpha-\frac{C_{22}h\cos\alpha}{s}u+\left(\frac{C_{23}h\cos\alpha}{s}-\frac{\left(C_{23}+C_{13}\right)h^{3}\cos\alpha}{3s^{3}}\right)v+\frac{C_{22}h\cos\alpha\cot\alpha}{s}w-\frac{C_{23}h\cot\alpha}{s}\frac{\partial u}{\partial\theta}\\ & +\left(\frac{C_{33}h^{3}}{3s^{3}}-\frac{C_{22}h}{s}+\frac{C_{22}h^{3}}{6s^{3}}+\frac{C_{12}h^{3}}{6s^{3}}\right)\cot\alpha\frac{\partial v}{\partial\theta}-C_{12}h\cos\alpha\frac{\partial u}{\partial s}+\left(\frac{C_{23}h^{3}\cos\alpha}{4s^{2}}-C_{23}h\cos\alpha+\frac{C_{13}h^{3}\cos\alpha}{3s^{2}}\right)\frac{\partial v}{\partial s}\\ & -\frac{\left(C_{23}+C_{13}\right)h^{3}}{3s^{3}}\frac{\partial w}{\partial\theta}+\frac{C_{22}h^{3}\sin\alpha}{12s^{2}}\frac{\partial w}{\partial s}-\frac{\left(C_{22}+2C_{12}+4C_{33}\right)h^{3}\cot\alpha}{12s^{2}}\frac{\partial^{2}v}{\partial s\partial\theta}+\frac{\left(C_{23}+C_{13}\right)h^{3}}{3s^{2}}\frac{\partial^{2}w}{\partial s\partial\theta}\\ & +\frac{\left(C_{12}+C_{22}+2C_{33}\right)h^{3}\csc\alpha}{6s^{3}}\frac{\partial^{2}w}{\partial\theta^{2}}-\frac{\left(C_{12}+2C_{33}\right)h^{3}\csc\alpha}{6s^{2}}\frac{\partial^{3}w}{\partial s\partial\theta^{2}}-\frac{\left(C_{23}+2C_{13}\right)h^{3}\cos\alpha}{12s}\frac{\partial^{2}v}{\partial s^{2}}\\ & +\left(N_{a}s_{1}\sin\alpha-\frac{C_{22}h^{3}\sin\alpha}{12s}\right)\frac{\partial^{2}w}{\partial s^{2}}+\frac{1}{6}C_{11}h^{3}\sin\alpha\frac{\partial^{3}w}{\partial s^{3}}-\frac{C_{23}h^{3}\cot\alpha\csc\alpha}{3s^{3}}\frac{\partial^{2}v}{\partial\theta^{2}}-\frac{C_{23}h^{3}\left(\csc\alpha\right)^{2}}{3s^{3}}\frac{\partial^{3}w}{\partial\theta^{3}}\\ & +\frac{C_{22}h^{3}\cot\alpha\left(\csc\alpha\right)^{2}}{12s^{3}}\frac{\partial^{3}v}{\partial\theta^{3}}+\frac{C_{22}h^{3}\left(\csc\alpha\right)^{3}}{12s^{3}}\frac{\partial^{4}w}{\partial\theta^{4}}+\frac{C_{23}h^{3}\cot\alpha\csc\alpha}{4s^{2}}\frac{\partial^{3}v}{\partial s\partial\theta^{2}}+\frac{C_{23}h^{3}\left(\csc\alpha\right)^{2}}{3s^{2}}\frac{\partial^{4}w}{\partial s\partial\theta^{3}}\\ & +\left(\frac{\left(C_{12}+2C_{33}\right)h^{3}\csc\alpha}{6s}\right)\frac{\partial^{4}w}{\partial s^{2}\partial\theta^{2}}+\frac{1}{3}C_{13}h^{3}\frac{\partial^{4}w}{\partial s^{3}\partial\theta}+\frac{1}{12}C_{13}h^{3}\cos\alpha\frac{\partial^{3}v}{\partial s^{3}}+\frac{\left(C_{12}+2C_{33}\right)h^{3}\cot\alpha}{12s}\frac{\partial^{3}v}{\partial s^{2}\partial\theta}+\frac{1}{12}C_{11}h^{3}s\sin\alpha\frac{\partial^{4}w}{\partial s^{4}}\end{aligned}\tag{B.13}$$

$$\begin{aligned}\underline{Eq3}^{NL}:\ & \frac{C_{23}h}{s^{2}}u\frac{\partial w}{\partial\theta}-\frac{C_{23}h}{s}\frac{\partial u}{\partial s}\frac{\partial w}{\partial\theta}-\frac{C_{33}h}{s^{2}}v\frac{\partial w}{\partial\theta}+\frac{C_{33}h}{s}\frac{\partial v}{\partial s}\frac{\partial w}{\partial\theta}+\frac{2C_{33}h}{s}v\frac{\partial^{2}w}{\partial s\partial\theta}-\frac{C_{23}h\cot\alpha}{s^{2}}w\frac{\partial w}{\partial\theta}\\ & +\frac{C_{23}h\cot\alpha}{s}\frac{\partial w}{\partial s}\frac{\partial w}{\partial\theta}+\frac{2C_{23}h\cot\alpha}{s}w\frac{\partial^{2}w}{\partial s\partial\theta}+\frac{\left(C_{33}-C_{22}\right)h\csc\alpha}{s^{2}}\frac{\partial u}{\partial\theta}\frac{\partial w}{\partial\theta}-\frac{2C_{33}h\csc\alpha}{s}\frac{\partial u}{\partial\theta}\frac{\partial^{2}w}{\partial s\partial\theta}\\ & -\frac{2C_{23}h\csc\alpha}{s}\frac{\partial v}{\partial\theta}\frac{\partial^{2}w}{\partial s\partial\theta}+\frac{C_{23}h\left(\csc\alpha\right)^{2}}{s^{3}}\left(\frac{\partial w}{\partial\theta}\right)^{3}-C_{13}h\frac{\partial w}{\partial\theta}\frac{\partial^{2}u}{\partial s^{2}}-C_{33}h\frac{\partial w}{\partial\theta}\frac{\partial^{2}v}{\partial s^{2}}\\ & -\left(C_{12}+C_{11}\right)h\sin\alpha\frac{\partial u}{\partial s}\frac{\partial w}{\partial s}-C_{12}h\sin\alpha u\frac{\partial^{2}w}{\partial s^{2}}+C_{13}h\sin\alpha v\frac{\partial^{2}w}{\partial s^{2}}+\frac{1}{2}C_{12}h\cos\alpha\left(\frac{\partial w}{\partial s}\right)^{2}\\ & +C_{12}h\cos\alpha w\frac{\partial^{2}w}{\partial s^{2}}-2C_{13}h\frac{\partial^{2}u}{\partial s\partial\theta}\frac{\partial w}{\partial s}-C_{13}h\frac{\partial u}{\partial\theta}\frac{\partial^{2}w}{\partial s^{2}}-\left(C_{12}+C_{33}\right)h\frac{\partial^{2}v}{\partial s\partial\theta}\frac{\partial w}{\partial s}-C_{12}h\frac{\partial v}{\partial\theta}\frac{\partial^{2}w}{\partial s^{2}}\\ & +\frac{\left(C_{12}+2C_{33}\right)h\csc\alpha}{2s^{2}}\left(\frac{\partial w}{\partial\theta}\right)^{2}\frac{\partial w}{\partial s}-\frac{\left(C_{12}+2C_{33}\right)h\csc\alpha}{2s}\left(\frac{\partial w}{\partial\theta}\right)^{2}\frac{\partial^{2}w}{\partial s^{2}}-C_{11}hs\sin\alpha\frac{\partial^{2}u}{\partial s^{2}}\frac{\partial w}{\partial s}\\ & -C_{11}hs\sin\alpha\frac{\partial u}{\partial s}\frac{\partial^{2}w}{\partial s^{2}}-C_{13}hs\sin\alpha\frac{\partial^{2}v}{\partial s^{2}}\frac{\partial w}{\partial s}-C_{13}hs\sin\alpha\frac{\partial v}{\partial s}\frac{\partial^{2}w}{\partial s^{2}}-3C_{13}h\frac{\partial w}{\partial\theta}\frac{\partial w}{\partial s}\frac{\partial^{2}w}{\partial s^{2}}\end{aligned}\tag{B.14}$$

$$\begin{aligned}
&-\frac{1}{2}C_{11}h\sin\alpha\left(\frac{\partial w}{\partial s}\right)^3-\frac{3}{2}C_{11}hs\sin\alpha\left(\frac{\partial w}{\partial s}\right)^2\frac{\partial^2 w}{\partial s^2}-\frac{C_{22}h\csc\alpha}{s^2}u\frac{\partial^2 w}{\partial\theta^2}+\frac{2C_{23}h\csc\alpha}{s^2}\frac{\partial v}{\partial\theta}\frac{\partial w}{\partial\theta}\\
&+\frac{C_{23}h\csc\alpha}{s^2}v\frac{\partial^2 w}{\partial\theta^2}+\frac{C_{22}h\cot\alpha\csc\alpha}{2s^2}\left(\frac{\partial w}{\partial\theta}\right)^2+\frac{C_{22}h\cot\alpha\csc\alpha}{s^2}w\frac{\partial^2 w}{\partial\theta^2}-\frac{C_{23}h\left(\csc\alpha\right)^2}{s^2}\frac{\partial^2 u}{\partial\theta^2}\frac{\partial w}{\partial\theta}\\
&-\frac{C_{23}h\left(\csc\alpha\right)^2}{s^2}\frac{\partial u}{\partial\theta}\frac{\partial^2 w}{\partial\theta^2}-\frac{C_{22}h\left(\csc\alpha\right)^2}{s^2}\frac{\partial^2 v}{\partial\theta^2}\frac{\partial w}{\partial\theta}-\frac{C_{22}h\left(\csc\alpha\right)^2}{s^2}\frac{\partial v}{\partial\theta}\frac{\partial^2 w}{\partial\theta^2}-3\frac{C_{22}h\left(\csc\alpha\right)^3}{2s^3}\left(\frac{\partial w}{\partial\theta}\right)^2\frac{\partial^2 w}{\partial\theta^2}\\
&-\frac{C_{12}h\csc\alpha}{s}\frac{\partial^2 w}{\partial\theta^2}\frac{\partial u}{\partial s}-\frac{\left(C_{12}+C_{33}\right)h\csc\alpha}{s}\frac{\partial w}{\partial\theta}\frac{\partial^2 u}{\partial s\partial\theta}-\frac{C_{23}h\csc\alpha}{s}\frac{\partial^2 w}{\partial\theta^2}\frac{\partial v}{\partial s}-\frac{2C_{23}h\csc\alpha}{s}\frac{\partial w}{\partial\theta}\frac{\partial^2 v}{\partial s\partial\theta}\\
&-\frac{C_{23}h}{s}\frac{\partial u}{\partial\theta}\frac{\partial w}{\partial s}-\frac{2C_{23}h}{s}u\frac{\partial^2 w}{\partial s\partial\theta}+\frac{C_{33}h}{s}\frac{\partial v}{\partial\theta}\frac{\partial w}{\partial s}-\frac{C_{33}h\csc\alpha}{s}\frac{\partial^2 u}{\partial\theta^2}\frac{\partial w}{\partial s}-\frac{C_{23}h\csc\alpha}{s}\frac{\partial^2 v}{\partial\theta^2}\frac{\partial w}{\partial s}\\
&-\frac{3C_{23}h\left(\csc\alpha\right)^2}{s^2}\frac{\partial w}{\partial\theta}\frac{\partial^2 w}{\partial\theta^2}\frac{\partial w}{\partial s}-\frac{3C_{23}h\left(\csc\alpha\right)^2}{s^2}\left(\frac{\partial w}{\partial\theta}\right)^2\frac{\partial^2 w}{\partial s\partial\theta}-2C_{13}h\frac{\partial u}{\partial s}\frac{\partial^2 w}{\partial s\partial\theta}-2C_{33}h\frac{\partial v}{\partial s}\frac{\partial^2 w}{\partial s\partial\theta}\\
&-\left(\frac{C_{12}h\csc\alpha}{2s}+\frac{C_{33}h\csc\alpha}{s}\right)\frac{\partial^2 w}{\partial\theta^2}\left(\frac{\partial w}{\partial s}\right)^2-\frac{\left(2C_{12}+4C_{33}\right)h\csc\alpha}{s}\frac{\partial w}{\partial\theta}\frac{\partial^2 w}{\partial s\partial\theta}\frac{\partial w}{\partial s}-3C_{13}h\left(\frac{\partial w}{\partial s}\right)^2\frac{\partial^2 w}{\partial s\partial\theta}
\end{aligned}\tag{B.14}$$

$$\begin{aligned}
\underline{BCsw}^{L}:&-\frac{\left(C_{23}+C_{13}\right)h^3\cos\alpha}{6s^2}v+\frac{\left(C_{12}+C_{22}+4C_{33}\right)h^3\cot\alpha}{12s^2}\frac{\partial v}{\partial\theta}-\frac{\left(C_{23}+C_{13}\right)h^3}{6s^2}\frac{\partial w}{\partial\theta}+\frac{C_{22}h^3\csc\alpha}{12s^2}\frac{\partial^2 w}{\partial\theta^2}\\
&+\frac{\left(C_{12}+4C_{33}\right)h^3\csc\alpha}{12s^2}\frac{\partial^2 w}{\partial\theta^2}+\frac{\left(C_{23}+2C_{13}\right)h^3\cos\alpha}{12s}\frac{\partial v}{\partial s}+\left(\frac{C_{22}h^3\sin\alpha}{12s}-\mathrm{N}_a\mathrm{s}_1\sin\alpha\right)\frac{\partial w}{\partial s}+\frac{C_{13}h^3}{6s}\frac{\partial^2 w}{\partial s\partial\theta}\\
&-\frac{1}{12}C_{11}h^3\sin\alpha\frac{\partial^2 w}{\partial s^2}-\frac{C_{23}h^3\cot\alpha\csc\alpha}{6s^2}\frac{\partial^2 v}{\partial\theta^2}-\frac{C_{23}h^3\left(\csc\alpha\right)^2}{6s^2}\frac{\partial^3 w}{\partial\theta^3}-\frac{\left(C_{12}+2C_{33}\right)h^3\cot\alpha}{12s}\frac{\partial^2 v}{\partial s\partial\theta}\\
&-\frac{\left(C_{12}+4C_{33}\right)h^3\csc\alpha}{12s}\frac{\partial^3 w}{\partial s\partial\theta^2}-\frac{1}{3}C_{13}h^3\frac{\partial^3 w}{\partial s^2\partial\theta}-\frac{1}{12}C_{13}h^3\cos\alpha\frac{\partial^2 v}{\partial s^2}-\frac{1}{12}C_{11}h^3s\sin\alpha\frac{\partial^3 w}{\partial s^3}
\end{aligned}\tag{B.15}$$

$$\begin{aligned}
\underline{BCsw}^{NL}:&\frac{C_{23}h}{s}u\frac{\partial w}{\partial\theta}-\frac{C_{33}h}{s}v\frac{\partial w}{\partial\theta}-\frac{C_{23}h\cot\alpha}{s}w\frac{\partial w}{\partial\theta}+\frac{C_{33}h\csc\alpha}{s}\frac{\partial u}{\partial\theta}\frac{\partial w}{\partial\theta}+\frac{C_{23}h\csc\alpha}{s}\frac{\partial v}{\partial\theta}\frac{\partial w}{\partial\theta}+\frac{C_{23}h\left(\csc\alpha\right)^2}{2s^2}\left(\frac{\partial w}{\partial\theta}\right)^3\\
&+C_{13}h\frac{\partial w}{\partial\theta}\frac{\partial u}{\partial s}+C_{33}h\frac{\partial w}{\partial\theta}\frac{\partial v}{\partial s}+C_{12}h\sin\alpha u\frac{\partial w}{\partial s}-C_{13}h\sin\alpha v\frac{\partial w}{\partial s}-C_{12}h\cos\alpha w\frac{\partial w}{\partial s}+C_{13}h\frac{\partial u}{\partial\theta}\frac{\partial w}{\partial s}\\
&+C_{12}h\frac{\partial v}{\partial\theta}\frac{\partial w}{\partial s}+\frac{\left(C_{12}+2C_{33}\right)h\csc\alpha}{2s}\left(\frac{\partial w}{\partial\theta}\right)^2\frac{\partial w}{\partial s}+C_{11}hs\sin\alpha\frac{\partial u}{\partial s}\frac{\partial w}{\partial s}+C_{13}hs\sin\alpha\frac{\partial v}{\partial s}\frac{\partial w}{\partial s}\\
&+\frac{3}{2}C_{13}h\frac{\partial w}{\partial\theta}\left(\frac{\partial w}{\partial s}\right)^2+\frac{1}{2}C_{11}hs\sin\alpha\left(\frac{\partial w}{\partial s}\right)^3
\end{aligned}\tag{B.16}$$

$$\begin{aligned}
\underline{BC\theta w}^{L}:&-\frac{C_{33}h^3\cot\alpha}{3s^3}v+\frac{C_{23}h^3\cot\alpha\csc\alpha}{3s^3}\frac{\partial v}{\partial\theta}-\frac{C_{33}h^3\csc\alpha}{3s^3}\frac{\partial w}{\partial\theta}+\frac{C_{23}h^3\left(\csc\alpha\right)^2}{3s^3}\frac{\partial^2 w}{\partial\theta^2}+\frac{C_{33}h^3\cot\alpha}{3s^2}\frac{\partial v}{\partial s}\\
&+\frac{\left(4C_{33}-C_{22}\right)h^3\csc\alpha}{12s^2}\frac{\partial^2 w}{\partial s\partial\theta}-\frac{\left(C_{13}+C_{23}\right)h^3}{6s}\frac{\partial^2 w}{\partial s^2}-\frac{C_{22}h^3\cot\alpha\left(\csc\alpha\right)^2}{12s^3}\frac{\partial^2 v}{\partial\theta^2}\\
&-\frac{C_{22}h^3\left(\csc\alpha\right)^3}{12s^3}\frac{\partial^3 w}{\partial\theta^3}-\frac{C_{23}h^3\cot\alpha\csc\alpha}{4s^2}\frac{\partial^2 v}{\partial s\partial\theta}-\frac{C_{23}h^3\left(\csc\alpha\right)^2}{3s^2}\frac{\partial^3 w}{\partial s\partial\theta^2}\\
&-\frac{\left(C_{12}+4C_{33}\right)h^3\csc\alpha}{12s}\frac{\partial^3 w}{\partial s^2\partial\theta}-\frac{1}{6}C_{13}h^3\frac{\partial^3 w}{\partial s^3}-\frac{C_{33}h^3\cot\alpha}{6s}\frac{\partial^2 v}{\partial s^2}
\end{aligned}\tag{B.17}$$

$$\begin{aligned}
\underline{BC\theta w}^{NL}:&\frac{C_{22}h\csc\alpha}{s^2}u\frac{\partial w}{\partial\theta}-\frac{C_{23}h\csc\alpha}{s^2}v\frac{\partial w}{\partial\theta}-\frac{C_{22}h\cot\alpha\csc\alpha}{s^2}w\frac{\partial w}{\partial\theta}+\frac{C_{23}h\left(\csc\alpha\right)^2}{s^2}\frac{\partial u}{\partial\theta}\frac{\partial w}{\partial\theta}+\frac{C_{22}h\left(\csc\alpha\right)^2}{s^2}\frac{\partial v}{\partial\theta}\frac{\partial w}{\partial\theta}\\
&+\frac{C_{22}h\left(\csc\alpha\right)^3}{2s^3}\left(\frac{\partial w}{\partial\theta}\right)^3+\frac{C_{12}h\csc\alpha}{s}\frac{\partial w}{\partial\theta}\frac{\partial u}{\partial s}+\frac{C_{23}h\csc\alpha}{s}\frac{\partial w}{\partial\theta}\frac{\partial v}{\partial s}+\frac{C_{23}h}{s}u\frac{\partial w}{\partial s}-\frac{C_{33}h}{s}v\frac{\partial w}{\partial s}-\frac{C_{23}h\cot\alpha}{s}w\frac{\partial w}{\partial s}\\
&+\frac{C_{33}h\csc\alpha}{s}\frac{\partial u}{\partial\theta}\frac{\partial w}{\partial s}+\frac{C_{23}h\csc\alpha}{s}\frac{\partial v}{\partial\theta}\frac{\partial w}{\partial s}+\frac{3C_{23}h\left(\csc\alpha\right)^2}{2s^2}\left(\frac{\partial w}{\partial\theta}\right)^2\frac{\partial w}{\partial s}+C_{13}h\frac{\partial u}{\partial s}\frac{\partial w}{\partial s}+C_{33}h\frac{\partial v}{\partial s}\frac{\partial w}{\partial s}\\
&+\frac{\left(C_{12}+2C_{33}\right)h\csc\alpha}{2s}\frac{\partial w}{\partial\theta}\left(\frac{\partial w}{\partial s}\right)^2+\frac{1}{2}C_{13}h\left(\frac{\partial w}{\partial s}\right)^3
\end{aligned}\tag{B.18}$$

$$\underline{BCsdw}:-\frac{C_{13}h^3\cos\alpha}{6s}v+\frac{C_{12}h^3\cot\alpha}{12s}\frac{\partial v}{\partial\theta}-\frac{C_{13}h^3}{6s}\frac{\partial w}{\partial\theta}+\frac{C_{12}h^3\csc\alpha}{12s}\frac{\partial^2 w}{\partial\theta^2}+\frac{1}{12}C_{13}h^3\cos\alpha\frac{\partial v}{\partial s}+\frac{1}{12}C_{12}h^3\sin\alpha\frac{\partial w}{\partial s}+\frac{1}{6}C_{13}h^3\frac{\partial^2 w}{\partial s\partial\theta}+\frac{1}{12}C_{11}h^3 s\sin\alpha\frac{\partial^2 w}{\partial s^2} \tag{B.19}$$

$$\underline{BC\theta dw}:-\frac{C_{23}h^3\cot\alpha\csc\alpha}{6s^3}v+\frac{C_{22}h^3\cot\alpha(\csc\alpha)^2}{12s^3}\frac{\partial v}{\partial\theta}-\frac{C_{23}h^3(\csc\alpha)^2}{6s^3}\frac{\partial w}{\partial\theta}+\frac{C_{22}h^3(\csc\alpha)^3}{12s^3}\frac{\partial^2 w}{\partial\theta^2}+\frac{C_{23}h^3\cot\alpha\csc\alpha}{12s^2}\frac{\partial v}{\partial s}+\frac{C_{22}h^3\csc\alpha}{12s^2}\frac{\partial w}{\partial s}+\frac{C_{23}h^3(\csc\alpha)^2}{6s^2}\frac{\partial^2 w}{\partial s\partial\theta}+\frac{C_{12}h^3\csc\alpha}{12s}\frac{\partial^2 w}{\partial s^2} \tag{B.20}$$

$$\underline{BCs\theta w}:-\frac{C_{33}h^3\cot\alpha}{3s^2}v+\frac{C_{23}h^3\cot\alpha\csc\alpha}{6s^2}\frac{\partial v}{\partial\theta}-\frac{C_{33}h^3\csc\alpha}{3s^2}\frac{\partial w}{\partial\theta}+\frac{C_{23}h^3(\csc\alpha)^2}{6s^2}\frac{\partial^2 w}{\partial\theta^2}+\frac{C_{33}h^3\cot\alpha}{6s}\frac{\partial v}{\partial s}+\frac{C_{23}h^3}{6s}\frac{\partial w}{\partial s}+\frac{C_{33}h^3\csc\alpha}{3s}\frac{\partial^2 w}{\partial s\partial\theta}+\frac{1}{6}C_{13}h^3\frac{\partial^2 w}{\partial s^2} \tag{B.21}$$

REFERENCES

[1] Bushnell D., 1982, Plastic buckling of various shells, *Jornal of Pressure Vessel Technology* **104**: 51-72.

[2] Jaskula L., Zielnica J., 2011, Large displacement stability analysis of elastic-plastic unsymmetrical sandwich cylindrical shells, *Thin-walled Structures* **49**: 611-617.

[3] Kouchakzadeh M.A., Shakouri M., 2015, Analytical solution for axisymmetric buckling of joined conical shells under axial compression, *Structural Engineering and Mechanics* **54**(4): 649-664.

[4] Lee W.S., Lin C.F., Liu T.J., 2006, Strain rate dependence of impact properties of sintered 316L stainless steel, *Journal of Nuclear Materials* **359**: 247-257.

[5] Naderi A.A., Rahimi G.H., Arefi M., 2014, Influence of fiber paths on buckling load of tailored conical shells, *Steel & Composite Structures* **16**(4): 375-387.

[6] Paczos P., Zielnica J., 2008, Stability of orthotropic elastic–plastic open conical shells, *Thin-Walled Structures* **46**: 530-540.

[7] Shakouri M., Spagnoli A., Kouchakzadeh M.A., 2016, Effects of imperfection shapes on buckling of conical shells under compression, *Structural Engineering and Mechanics* **60**(3): 365-386.

[8] Soedel W., 2004, *Vibrations of Shells and Plates*, Marcel Dekker Inc., New York, USA.

[9] Washizu K., 1975, *Variational Methods in Elasticity and Plasticity*, Pergamon Press, Oxford, UK.

[10] Zielnica J., 1981, Elastic plastic buckling of sandwich conical shells under axial compression, *Bulletin de l'Académie Polonaise des Sciences / Série des Sciences Techniques* **29**: 239-251.

[11] Zielnica J., 2003, Non-linear stability of elastic–plastic conical shell under combined load, *Journal of Theoretical and Applied Mechanics* **41**: 693-709.

[12] Zielnica J., 2012, Buckling and stability of elastic-plastic sandwich conical shells, *Steel & Composite Structures* **13**(2): 157-169.